Cancer Chemother Pharmacol (2011) 68:959–970
DOI 10.1007/s00280-011-1565-4

ORIGINAL ARTICLE

A phase I study of MN-029 (denibulin), a novel vascular-disrupting agent, in patients with advanced solid tumors

Alejandro D. Ricart · Edward A. Ashton · Matthew M. Cooney · John Sarantopoulos · Joanna M. Brell · Maria A. Feldman · Kale E. Ruby · Kazuko Matsuda · Mark S. Munsey · Gerardo Medina · Angela Zambito · Anthony W. Tolcher · Scot C. Remick

Received: 24 August 2010 / Accepted: 16 January 2011 / Published online: 9 February 2011

Abstract
Purpose MN-029 (denibulin HCl) is a novel vascular-disrupting agent that reversibly inhibits microtubule assembly, resulting in disruption of the cytoskeleton of tumor vascular endothelial cells. This study determined the safety, pharmacokinetics, and acute anti-vascular effects of MN-029.
Methods Patients were treated with escalating doses of MN-029 (4.0–225 mg/m^2) administered IV at 3-week intervals. This first-in-human study followed an accelerated titration design, with intra-patient dose escalation. Plasma samples were assayed to determine PK parameters. DCE-MRI scans were acquired at baseline and at 6–8 h post-dose.
Results Thirty-four patients received 151 infusions of MN-029. The most common toxicities of MN-029 included nausea and vomiting (which appeared to be dose related), diarrhea, fatigue, headache, and anorexia. No clinically significant myelotoxicity, stomatitis or alopecia was observed. There was no evidence of cumulative toxicity in patients receiving multiple courses of therapy. The cohort at 180 mg/m^2 was expanded to six patients due to a reversible episode of acute coronary ischemia, without sequelae and with preservation of myocardial function. Two dose-limiting toxicities occurred at 225 mg/m^2, a transient ischemic attack and grade 3 transaminitis, thus ending dose escalation. Pharmacokinetic data indicated dose-related increases in C_{max} and AUC values, although substantial inter-subject variability was observed. No objective responses were noted; however, five patients had stable disease ≥6 months. A significant linear correlation was found between reduction in K^{trans} and exposure to MN-029.
Conclusions MN-029 was generally well tolerated and showed decrease in tumor vascular parameters. The maximum tolerated dose was 180 mg/m^2.

Keywords MN-029 · Vascular-disrupting agent · Phase I

Presented in part at the 42nd Annual Meeting of the American Society of Clinical Oncology, June 2–6, 2006, Atlanta, GA and at the 18th European Organization for Research and Treatment of Cancer-National Cancer Institute-American Association for Cancer Research Symposium on Molecular Targets and Cancer Therapeutics, November 7–10, 2006, Prague, Czech Republic.

A. D. Ricart · J. Sarantopoulos · G. Medina · A. W. Tolcher
Institute for Drug Development, Cancer Therapy and Research Center, San Antonio, TX, USA

E. A. Ashton
VirtualScopics, Inc., Rochester, NY, USA

M. M. Cooney · A. Zambito · S. C. Remick
Developmental Therapeutics Program, CASE Comprehensive Cancer Center, Cleveland, OH, USA

J. M. Brell
Division of Cancer Prevention, National Cancer Institute, Bethesda, MD, USA

M. A. Feldman · K. E. Ruby · K. Matsuda · M. S. Munsey
MediciNova, Inc., San Diego, CA, USA

A. D. Ricart (✉)
Oncology Development, Pfizer Inc., 10646, Science Center Drive, San Diego, CA 92121, USA
e-mail: alejandro.d.ricart@pfizer.com

Introduction

Targeted therapy of the tumor vascular compartment has been recently validated [1–5]. Vascular-disrupting agents (VDAs) are emerging as promising new therapies that

preferentially target pre-existing tumor blood vessels [6–8]. Tumor blood vessels are irregularly formed, lack stromal support and are highly dependent on their tubulin cytoskeleton to maintain their structural integrity [8–10]. Because the target of the VDAs is a normal diploid endothelial cell, it is unlikely to acquire genetic mutations that render these cells drug resistant [8–10]. In this respect, VDAs differ from anti-angiogenic agents that prevent new blood vessel formation rather than disrupt pre-existing tumor blood vessels. Potential pharmacodynamic markers of biologic activity, i.e., blood flow and perfusion, are measurable in the clinic using dynamic contrast-enhanced magnetic resonance imaging (DCE-MRI) [11–15]. Of note, temporary shutdown of tumor blood supply can produce significant effect; well-designed studies indicate that >99% of tumor cells can be killed in vivo during a 2-h period of ischemia [8, 16]. Consequently, unlike anti-angiogenic agents, VDAs should require only intermittent administration with additive or synergistic anti-tumor effects to conventional treatments rather than chronic administration over months or years [17].

MN-029 (denibulin HCl; methyl-6-[(4-{[(2S)-2-aminopropanoyl]amino} phenyl)thio]-1*H*-benzimidazol-2-ylcarbamate hydrochloride) is a novel VDA with a unique chemical structure. MN-029 is rapidly metabolized via amide bond hydrolysis to form MN-022. MN-022 is subsequently N-acetylated to form MN-021 [18]. Both MN-029 and MN-022 inhibit the growth of MDA-MB-435 breast carcinoma and human umbilical-vein endothelial cells (HUVEC) at nM concentrations, but require μM concentrations (>1,000-fold increase) to produce cytotoxicity. MN-029, MN-022, and MN-021 bind reversibly to the colchicine-binding site on tubulin and inhibit microtubule assembly, resulting in disruption of the cytoskeleton of tumor endothelial cells (EC). This effect ultimately leads to a temporary reduction in tumor blood flow. As with other VDAs, MN-022 inhibits capillary tube formation in vitro in proliferating EC, such as stimulated HUVECs, but lacks significant effects on resting (confluent) EC [18].

Xenograft studies demonstrated that single doses of MN-029 produce, in a dose-dependent manner, loss of blood flow and consequent widespread necrosis of tumors; repeated administration results in significant tumor growth inhibition [18, 19]. When used in combination with radiation therapy or cisplatin chemotherapy, MN-029 significantly enhanced tumor killing compared to that seen with radiation or cisplatin alone [19]. Toxicology studies in rats and dogs were consistent with inhibition of tubulin polymerization. Consequently, bone marrow, testes, and lymphoid tissues were identified as target organs. Toxicities were generally dose-related in incidence and severity and reversible within 2 weeks. No histopathologic evidence of neurotoxicity or cardiovascular toxicity was observed in these studies [18]. Toxicology testing supported a starting dose for clinical trials of 4 mg/m^2.

The rationale for the clinical development of MN-029 included its significant activity in a broad spectrum of experimental tumors at non-toxic doses and the potential to enhance the effects of cytotoxic chemotherapy, radiotherapy, and anti-angiogenic therapy. The principal objectives of this first phase I study were to determine (1) the maximum tolerated dose (MTD) of MN-029, (2) its clinical safety profile, (3) the pharmacokinetics of MN-029 and its metabolites MN-022 and MN-021, and (4) the effects of MN-029 administration on tumor blood flow using DCE-MRI. This study also evaluated preliminary anticancer activity of MN-029 in patients with advanced solid malignancies.

Patients and methods

Patient selection

Patients with pathologically confirmed solid malignancies refractory to standard therapy or for whom no standard therapy existed were eligible to participate in the study. Eligibility criteria also included the following: age ≥ 18 years, life-expectancy ≥ 12 weeks, an Eastern Cooperative Oncology Group (ECOG) performance status of 0–2, previous systemic therapy ≥ 4 weeks (6 weeks for prior mitomycin C or a nitrosourea), hemoglobin ≥ 9 g/dL, absolute neutrophil count (ANC) ≥ 1,500/μL, platelet count ≥ 100,000/μL, bilirubin ≤ 1.5 mg/dL, aspartate serum transferase (AST) and alanine serum transferase (ALT) ≤ 3 times the upper limit of normal (ULN), serum creatinine ≤ 1.5 times the ULN, measurable disease, no evidence of active brain metastases, no evidence of HIV seropositivity, and no coexisting severe medical conditions or anticoagulation therapy. Finally, because of the potential effects of MN-029 on vasculature, patients with a history of any bleeding disorder, thromboembolic events, or major surgical procedure within 4 weeks of treatment were also excluded. Patients gave written informed consent according to federal and institutional guidelines before treatment.

Study design and treatment

MN-029 was administered intravenously (IV) over 10 min (or at 2 mL/min, if the dose volume was >20 mL), at dose levels of 4.0–225 mg/m^2 every 3 weeks. An accelerated titration design was used initially [20], and patients were allowed to receive an escalated dose after three courses of treatment if they experienced no drug-related toxicity of grade ≥2, and there had been fewer than two instances of ≥grade 2 toxicity (except for nausea or vomiting) at the

next dose level. If one patient experienced a dose-limiting toxicity (DLT), the cohort was expanded to six patients. The MTD was defined as the highest dose at which <4 of up to 12 patients experienced a treatment-related DLT. DLT was defined during course 1 as grade 3–4 neutropenia associated with fever (38.5°C), grade 4 neutropenia ≥ 7 days, thrombocytopenia <25,000/μL, nausea, vomiting, or diarrhea ≥grade 3 despite the use of adequate/maximal medical intervention and/or prophylaxis, or any other non-hematologic toxicity ≥grade 3. Toxicity was graded according to the National Cancer Institute's (NCI) Common Toxicity Criteria for Adverse Events (CTCAE), Version 3.0. A patient's dose was reduced by 25% (a maximum of two dose reductions were allowed) if a DLT was reached in an individual patient.

MN-029 was supplied in 50-mg (10 mL) and 100-mg (20 mL) single-use vials by MediciNova, Inc. (San Diego, CA). The dose was administered in a fixed total volume of 20 mL by adding sodium chloride for injection USP (0.9%) when the volume of MN-029 was <20 mL.

Safety assessments

A complete medical history, physical examination, concurrent medication profile, and routine laboratory studies were performed pre-treatment and on day 8 of every course. Routine laboratory studies included a complete blood count, differential white blood count, prothrombin time, partial thromboplastin time, serum chemistry including electrolytes, BUN, creatinine, glucose, alkaline phosphatase, ALT, AST, total bilirubin, albumin, calcium, magnesium, phosphorus, lactate dehydrogenase, and urinalysis. Pre-treatment assessments also included an ECG, relevant radiologic studies, and tumor markers. Radiologic studies for disease status were performed every 9 weeks. Response was assessed by RECIST criteria [21].

Pharmacokinetic assessments

Plasma samples were collected at the following time points during course 1 of therapy: pre-dose, immediately before the end of infusion, 5, 15, 30, and 45 min and 1, 1.5, 2, 4, 6, 10, 18, and 24 h following the completion of the infusion. Urine specimens were also collected immediately before the first dose, and for 24 h after the completion of the first infusion; but these samples were not analyzed as long-term frozen stability of MN-029 and MN-022 in urine (to cover the duration that the study samples were stored) could not be established.

Each plasma sample was analyzed for levels of MN-029, MN-022, and MN-021 using a validated liquid chromatography/mass spectrometry/mass spectrometry (LC–MS/MS) assay with a lower limit of quantitation (LLOQ) of 0.2 ng/mL. Briefly, calibration standard solutions were added to 100 μL of fortified plasma (containing 20 μM amastatin hydrochloride to prevent degradation) in a 96-well plate to yield final concentrations of 0.6, 7.5, 15, 30, 75, and 150 ng/mL of MN-029, MN-022, and N-acetyl MN-022. Quality control (QC) samples were prepared in monkey plasma containing 0.2, 0.6, 60, and 120 ng/mL of each analyte. Fifty microliters of internal standard (IS; 25 ng/mL verapamil) were added to each well. Methanol (400–550 μL) was added to the calibration standard, QC, blank plus IS, and true blank wells to precipitate plasma proteins. The 96-well plate was capped and vortex for ~5 min at 3,000 rpm to sediment precipitated proteins. An aliquot (350 μL) of the supernatant was transferred from each well to a clean 96-well plate using a TOMTEC Quadra 96®. The plate was capped and centrifuged for ~3 min at 3,000 rpm. The plate was then loaded in the autosampler (a Leap Injector, HTC PAL) maintained at ambient temperature. An aliquot (8 μL) was injected onto the LC–MS/MS system (a Shimadzu LC-10Advp with a Micromass Triple Quadrupole MS) with column switching. Separation was achieved using a Sepax C8 column (2.1 mm ID × 50 mm, 5 μm; Sepax Technologies). Mobile phase consisted of water/20 mM ammonium formate, pH 2 (90:10, v/v; mobile phase A) and methanol/acetronitrile/20 mM ammonium phosphate, pH 2.5 (50:50:5, v/v; mobile phase B). The following gradient was employed: time zero—20% B; time 3 min—100% B over 3 min; and time 6.1 min—20% B. Flow rate was ~400 μL/min. Total run time was ~7.5 min. MN-029 (retention time = 1.81 min), MN-022 (retention time = 2.04 min), and N-acetyl MN-022 (retention time = 2.32 min) concentrations were quantified by positive ion MS/MS with multiple reaction monitoring (MRM). Transitions monitored were 386.0 → 314.9 m/z for MN-029, 315.0 → 124.0 m/z for MN-022, 356.9 → 189.9 m/z for N-acetyl MN-022, and 455.3 → 164.9 m/z for IS. Calibration curves were obtained by performing a linear regression analysis of peak area ratios versus concentration using a $1/x^2$ weighting factor. Details regarding the validation are provided in Appendix (as a supplement).

The individual plasma concentration data sets were analyzed by a non-compartment, constant-infusion administration model using WinNonLin™ version 4.1 (Pharsight Corp., Mountain View, CA).

Pharmacodynamic assessments

DCE-MRI data were acquired at baseline and at 6–8 h post-dose on day 1 of the first course of therapy. A 5-slice, 5-cm slab was imaged in each case, with spatial resolution of 2 mm in-plane and 10 mm between images. Images were acquired in the coronal plane using a semi-keyhole

technique, with TE/TR/TI/FA of 2.42/1000/340/16 and temporal resolution of approximately 3 s per slab. Contrast was delivered via a power injector at a dose of 2 mM/kg. Each DCE-MRI slab was intended to contain at least one target lesion suitable for analysis. In this study, target lesions were required to be at least 2 cm in diameter when located in regions not strongly affected by respiratory motion (for example, the pelvis) and 3 cm in diameter when located in regions such as the liver or lungs, which are more strongly affected by respiratory motion. Target lesions were required to not be significantly calcified and to show noticeable contrast uptake at baseline. Cystic lesions were avoided.

This study made use of a previously described data-derived arterial input function (AIF) method [22]. Vascular parameters were calculated using previously described methods [23]. The parameters of primary interest in this work were the volume transfer constant between blood plasma and extra-cellular, extra-vascular space, commonly referred to as K^{trans} [24], and the blood-normalized area under the tumor enhancement curve over the first 90 s post-injection ($IAUCBN_{90}$) [24, 25]. K^{trans} is related to both blood flow (F) and endothelial permeability-surface area product (PS) and is therefore a good endpoint for assessing the blood supply to a target lesion. $IAUCBN_{90}$, which depends on the fractional volume of extra-vascular extra-cellular space (EES) in addition to F and PS, is in general highly correlated with K^{trans}. However, it is not dependent on any physiologic model and is therefore in some cases less sensitive to noise and data irregularities.

The results of these calculations were assessed in several ways. First, the K^{trans} and $IAUCBN_{90}$ values derived for the 10 patients who received lower doses ($\leq$54 mg/m^2) of MN-029 were used to estimate scan–rescan variability for this analysis system in the absence of biologically active treatment. Coefficients of variability (CoV) were estimated for each patient by calculating the standard deviation of the parameter values calculated at the pre- and post-dose imaging sessions and dividing this value by the mean of the two values. This value is unbiased. However, we were attempting to estimate the expected value of the CoV for this population. This value would be biased low due to the small number of samples ($n = 2$) used to calculate each individual CoV and must be multiplied by a factor K, which is a nonlinear function of n. For $n = 2$, the bias is $K = 1.25331$. Therefore, an accurate estimate of the expected value of the CoV was obtained by multiplying each individual CoV by K and then finding the mean value of the resulting distribution [23].

An assessment of evidence of statistically significant vascular disruption was carried out using parameter values calculated for the 12 patients receiving biologically active doses ($\geq$120 mg/m^2) of MN-029. Evidence was evaluated both on an individual basis and on a cohort basis. Individual patients were evaluated for objective vascular response (OVR)—a reduction in vascular parameters greater than twice the CoV defined in the low-dose analysis. Group changes in the 12 biologically active dose patients were assessed in two ways. First, the 95% confidence interval (CI) on mean change in each vascular parameter was calculated. If a significant treatment effect was to be present in a given group, the upper bound of the 95% CI should be less than 0. Second, a Student's t-test was used to determine whether there were significant differences between the biologically active dose group and the low-dose group. Finally, all subjects were used to assess the relationship between AUC_{0-24h} for MN-029 and the measured vascular parameters. In the presence of a dose-dependent vascular effect, we would expect these parameters to be significantly negatively correlated.

Results

Patient characteristics

Thirty-four patients, whose pertinent demographic characteristics are displayed in Table 1, received a total of 151 infusions of MN-029 at dose levels ranging from 4 to 225 mg/m^2. The total number of new patients treated and the number of courses at each dose level, as well as the overall dose-escalation scheme, are depicted in Table 2. Twenty-six patients (76%) and 18 patients (53%) completed 2 and at least three courses of therapy, respectively. The initial dose level was reduced in five patients.

Safety and tolerability

Table 3 shows adverse events, at least possibly related to MN-029 occurring in any course of treatment, that were reported with $\geq$10% frequency. In this table, the highest grade of an event per individual patient was recorded. The most common toxicities of MN-029 were characteristic of other VDAs and included nausea and vomiting (which appeared to be dose related), diarrhea, fatigue, headache, and anorexia. However, there were no clinically significant changes in median systolic/diastolic blood pressure or ECG parameters. Routine antiemetic pre-medication was instituted starting at 80 mg/m^2 dose due to moderate nausea. There was no significant myelotoxicity, stomatitis, or alopecia. Nine patients received more than three courses of therapy without evidence of cumulative toxicity.

The 16 mg/m^2 cohort was expanded because of grade 2 possibly drug-related diarrhea. Dose escalation proceeded until an initial DLT was observed at the 180 mg/m^2 cohort, consisting of an episode of reversible acute coronary

Table 1 Patient characteristics

Characteristics	No.
No. of patients	34
Median age (range) in years	57 (34–76)
Sex (M/F)	17/17
Median no. of courses/patient (range)	3 (1–36)[a]
Performance status (ECOG)	
0	15
1	16
2	3
Previous therapy	
Chemotherapy	30
Median no. (range)	3 (0–6)
Radiotherapy	14
Tumor types	
Colorectal	7
Renal cell carcinoma	6
Carcinoid	4
Soft-tissue sarcoma	3
Hepatocellular carcinoma	3
Ovarian	2
Melanoma	2
Others[b]	7

[a] Four patients were ongoing at the cut-off date and were still receiving extended courses of study drug when transitioned to physician-sponsored compassionate use programs

[b] Pancreatic, urethral, anaplastic thyroid, head and neck, non-small-cell lung cancer, adenocarcinoma of unknown primary site, and gastrinoma

ischemia. The patient had moderate nausea and vomiting approximately 90 min after the infusion that responded to anti-emetic medication. An ECG 3 h post-infusion showed ST segment depression in inferior leads, improving at 4 h post-infusion. The ST segment depression completely resolved at 24 h, but a new T-wave inversion pattern was noted in the lateral leads. No new Q-wave was noted. A follow-up echocardiogram showed normal left ventricular function, with no evidence of focal wall motion abnormalities. An exercise stress test confirmed normal exercise tolerance with no exercise-induced ischemia. A cardiac catheterization demonstrated normal coronary anatomy, except for 40% stenosis of the proximal left anterior descending coronary artery. Therefore, this cohort was expanded to six patients with no further DLTs observed.

Two out of four patients had DLTs at 225 mg/m^2, a grade 3 transaminitis and a transient ischemic attack. The

Table 3 MN-029 treatment-related adverse events (reported ≥10% frequency)

Adverse events	CTCAE grade n (%)				
	1	2	3	4	5
Vomiting	11 (32)	3 (9)	2 (6)	0	0
Nausea	6 (18)	6 (18)	2 (6)	0	0
Diarrhea	4 (12)	4 (12)	2 (6)	0	0
Fatigue	2 (6)	7 (21)	0	0	0
Headache	6 (18)	1 (3)	0	0	0
Anorexia	5 (15)	1 (3)	0	0	0

Table 2 MN-029 treatment by dose level and DLT

Dose level (mg/m^2)	No. of patients treated ($N = 34$)			Total no. of courses	No. of patients with DLT
	New	Dose escalated	Total		
4	1	–	1	3	0/1
8	1	–	1	6	0/1
16	5	1	6	16[a]	0/5
24	3	2	5	12[b]	0/3
36	3	2	5	12	0/3
54	3	3	6	15	0/3
80	3	4	7	28[c]	0/3
120	3	3	6	17	0/3
180	8	2	10	36	1/8[e]
225	4	–	4	6[d]	2/4[f]

[a] Two cycles at 12 mg/m^2

[b] One cycle at 18 mg/m^2

[c] Three cycles at 60 mg/m^2

[d] One cycle at 165 mg/m^2

[e] A reversible episode (3 h post-dose) of acute coronary ischemia (without sequelae and with preservation of myocardial function)

[f] One patient had a transient ischemic attack without sequelae and another patient had G3 transaminitis

transaminitis occurred in a patient with a diagnosis of carcinoid tumor with hepatic metastasis. His liver function tests returned to baseline and he received a second course of therapy at 165 mg/m^2. MN-029 was discontinued after recurrent transaminitis, although this new episode was also reversible, without consequences on the liver function. The neurologic presentation consisted of mild reversible aphasia 1 h after the infusion with the patient being normotensive. An immediate CT scan, cardiac enzyme panel, chest X-ray, ECG, and a follow-up MRI were unremarkable. The patient was discharged to home in less than 24 h. Dose escalation ended at this point, and a total of 10 patients were evaluated at 180 mg/m^2 without additional DLT.

Pharmacokinetics

Thirty-four patients had plasma sampling performed in the first course of therapy (33 patients had sampling at all time points). MN-029 is metabolized to the free amine, MN-022, which is N-acetylated to MN-021. However, the metabolic pathways for MN-029 metabolism to MN-022 and N-acetyl MN-022 (MN-021) have not yet been elucidated. MN-029 and MN-022 inhibit cellular growth (read *introduction* section for details). It is not known whether the activity observed in cell cultures is due to conversion to MN-022 or due to direct activity, but MN-029 is less potent than MN-022 in vitro. The mean non-compartmental pharmacokinetic variable estimates at each dose level are listed in Table 4. Linear regression analysis of MN-029, MN-022, and MN-021 plasma area under the curve from time 0 to infinity ($AUC_{0-\infty}$) versus dose are shown in Fig. 1a–c. Inter-patient variation in pharmacokinetics was large, as shown in these figures of individual $AUC_{0-\infty}$ values as a function of dose. In general, C_{max} and $AUC_{0-\infty}$ values increased with increasing doses, and the overall $AUC_{0-\infty}$ appeared to be dose proportional. The mean clearance of MN-029 ranged from 76.0 to 166.5 L/h/m^2 between 54 and 225 mg/m^2 doses and did not appear to decrease with increasing dose (Table 4).

The C_{max} of MN-029 was reached in most patients between 0.2 and 0.3 h after the initiation of the IV infusion of doses from 4 to 54 mg/m^2. For higher dose levels of 120 to 225 mg/m^2, C_{max} was achieved later due to longer infusion times. Following attainment of peak concentrations, individual concentration–time profiles revealed multiple phases (multi-exponential decay). The mean apparent half-lives ($t_{1/2}$) based on blood sampling up to 24 h appeared to be dependent on dose. For dose levels of 4–36 mg/m^2, the mean $t_{1/2}$ ranged from 0.1 to 1.4 h. For dose levels of 54–225 mg/m^2, mean $t_{1/2}$ was significantly longer and ranged from $\sim$4 to 12 h (except for the cohort at 80 mg/m^2 based on data from a single patient).

The conversion of MN-029 to MN-022 was rapid. The C_{max} and $AUC_{0-\infty}$ for MN-022 generally increased with increasing dose. Plasma concentrations of MN-022 were substantially higher than those of MN-029; the AUC_{0-24h} for MN-022 was 3.3 to 23.3 times higher than that of MN-029. The mean $t_{1/2}$ ranged from 1.9 to 7.0 h and appeared to be dependent on dose. Half-lives for MN-022 were longer than those of MN-029 at all dose levels except 120 and 180 mg/m^2.

The $AUC_{0-\infty}$ values for MN-021 were greater than those of MN-029, but less than those of MN-022. In addition, the half-lives of MN-021 were longer than those of MN-029 at dose levels of 4 to 36 mg/m^2.

Antitumor activity

There were no complete or partial responses. Nine patients had stable disease after three courses of therapy. Of note, five patients achieved prolonged stable disease of $\geq$6 months (carcinoid tumor = 2, melanoma = 2, pancreatic cancer = 1). Four patients were on therapy at the data cut-off date, including three patients with carcinoid tumor (+18, +16, and +3 months) and one patient with melanoma (+6 months). DCE-MRI data were not available for two patients with carcinoid tumor. Cumulative exposure (phase I and the extension study) to MN-029 range from 27 to 45 courses of therapy for these four patients, with only one patient discontinuing therapy due to progressive disease.

Pharmacodynamic assessment

Of the 25 imaged patients, 24 had suitable target lesions and were deemed analyzable, while one did not and was excluded. No patient data sets were excluded due to technical issues or acquisition errors. Reproducibility results for both K^{trans} and $IAUCBN_{90}$ for the 10 low-dose patients are given in Table 5. Percent CoV for K^{trans} and $IAUCBN_{90}$ based on these data were 8.7 and 8.8%, respectively. Pre- and post-dose values for K^{trans} and $IAUCBN_{90}$ for each of the 12 analyzable patients receiving doses of MN-029 $\geq$120 mg/m^2 are also shown in Table 5.

Based on the reproducibility data shown in Table 5 and previously published reproducibility results using this analysis system, a reduction in either K^{trans} or $IAUCBN_{90}$ of 20% or more can be considered evidence of OVR. By this criterion, six of the twelve patients receiving doses of MN-029 $\geq$120 mg/m^2 achieved OVR in at least one of their target lesions. Note that two of these six patients had a second analyzed lesion that showed a smaller, non-significant reduction in vascular parameters. Note also that none of the twelve patients receiving doses of MN-029 $\leq$80 mg/m^2

Table 4 MN-029, MN-022, and MN-021 non-compartmental PK parameters

Dose level (mg/m^2)	Compound	No. of patients	Mean values (±SD)						
			$t_{1/2}$ (h)	C_{max} (ng/mL)	T_{max} (h)	$AUC_{0-\infty}$ (h.ng/mL)	CL ($L/h/m^2$)	V_z (L/m^2)	$AUC_{(0-\infty)}$/dose
4	MN-029	1	0.1	131	0.2	27.6	144.7	13.3	6.9
	MN-022	1	3.7	167	0.3	395	–	–	98.8
	MN-021	1	3.9	35.6	1.2	187	–	–	46.8
8	MN-029	1	0.1	551	0.3	94.2	84.9	15.7	11.8
	MN-022	1	1.9	289	0.2	321	–		40.1
	MN-021	1	2.0	42.9	0.4	116	–	–	14.5
16	MN-029	5	0.5 (0.2)	1,091 (430)	0.2 (0.0)	163 (32)	101.3 (19.9)	72.7 (33.5)	10.2 (2.0)
	MN-022	5	4.3 (0.6)	788 (388)	0.2 (0.1)	1,823 (518)	–	–	113.9 (32.4)
	MN-021	5	4.0 (0.6)	112 (50)	0.7 (0.4)	598 (299)	–	–	37.4 (18.7)
24	MN-029	3	0.4 (0.2)	833 (219)	0.3 (0.1)	137 (38)	184.3 (51.0)	91.3 (32.7)	5.7 (1.6)
	MN-022	3	5.3 (2.6)	662 (200)	0.2 (0.2)	1,885 (548)	–	–	78.5 (22.8)
	MN-021	3	3.7 (0.2)	114 (29)	1.0 (0.3)	593 (277)	–	–	24.7 (11.5)
36	MN-029	3	1.4 (1.0)	2,171 (1,727)	0.2 (0.0)	332 (240)	252.5 (302.9)	303.6 (198.1)	9.2 (6.7)
	MN-022	3	5.5 (1.2)	1,331 (316)	0.2 (0.0)	2,657 (1,051)	–	–	73.8 (29.2)
	MN-021	3	4.2 (1.3)	194 (95)	1.5 (0.8)	1,292 (1,027)	–	–	35.9 (28.5)
54	MN-029	3	4.0 (NC)	3,714 (1,794)	0.2 (0.0)	751 (NC)	76.3 (NC)	430.7 (NC)	13.9 (NC)
	MN-022	3	5.1 (1.4)	1,572 (646)	0.2 (0.1)	5,014 (2,591)	–	–	92.9 (48)
	MN-021	3	3.9 (1.3)	274 (172)	0.9 (0.3)	1,905 (1,674)	–	–	35.3 (31)
80	MN-029	3	1.9 (NC)	6,847 (1,931)	0.2 (0.1)	998 (NC)	80.2 (NC)	225 (NC)	12.5 (NC)
	MN-022	3	5.2 (0.8)	2,796 (499)	0.3 (0.0)	12,349 (3,538)	–	–	154.4 (44.2)
	MN-021	3	5.2 (0.9)	491 (246)	0.9 (0.3)	3,893 (1,244)	–	–	48.7 (15.6)
120	MN-029	3	12.1 (NC)	4,023 (1,418)	0.4 (0.1)	1,110 (NC)	117.8 (NC)	2,095.5 (NC)	9.3 (NC)
	MN-022	3	5.4 (2.2)	3,863 (161)	0.4 (0.0)	20,779 (17,173)	–	–	173.2 (143.1)
	MN-021	3	5.3 (2.3)	390 (146)	2.9 (3.0)	4,080 (3,804)	–	–	34 (31.7)
180	MN-029	8	7.3 (5.2)	4,069 (1,229)	0.6 (0.1)	1,346 (503)	166.5 (110.5)	2,127.2 (2,445.4)	7.5 (2.8)
	MN-022	8	7.0 (2.6)	6,143 (471)	0.8 (0.1)	41,535 (16,406)	–	–	230.8 (91.1)
	MN-021	8	6.4 (2.2)	975 (484)	2.2 (0.4)	10,856 (6,073)	–	–	60.3 (33.7)
225	MN-029	4	4.6 (2.8)	7,253 (3,253)	0.7 (0.1)	3,127 (846)	76.0 (20.2)	462.4 (283.4)	13.9 (3.8)
	MN-022	4	6.7 (1.3)	10,160 (1,838)	0.8 (0.2)	69,198 (3,743)	–	–	307.5 (16.6)
	MN-021	4	6.3 (1.2)	2,248 (780)	3.0 (1.1)	24,713 (10,263)	–	–	109.8 (45.6)

NC not calculated since there were less than 3 pharmacokinetically evaluable patients

achieved OVR. Mean change in K^{trans} from pre- to post-dose imaging in the low-dose ($\leq$54 mg/m^2) group was +9.1% (95% CI: −0.2 to +18%) and in the biologically active dose ($\geq$120 mg/m^2) group was −14.4% (95% CI: −22 to −6.9%). The difference between these groups was statistically significant ($P < 0.0001$). Mean change in IAUCBN$_{90}$ from pre- to post-dose imaging in the low-dose group was +7.5% (95% CI: −3.1 to +18%) and in the biologically active dose group was −16% (95% CI: −25 to −7.3%). The difference between these groups was also significant ($P = 0.002$). The patient who showed the maximum K^{trans} reduction (−37%) had a maximum target lesions regression of 19% by RECIST.

Figure 2a shows a scatter plot comparing change in K^{trans} to AUC_{0-24h} for MN-029. All analyzable patients from all dose cohorts are represented. Each of the three subjects with more than one analyzed lesion is represented by the stronger responding lesion. These parameters are negatively correlated, as expected, with $R^2 = 0.45$. This correlation is significant ($P < 0.001$). Figure 2b shows a similar scatter plot comparing change in IAUCBN$_{90}$ to AUC_{0-24h} for MN-029. Although the trend seen here is similar to that in Fig. 1c, the data scatter is greater and the correlation is correspondingly weaker ($R^2 = 0.16$). This correlation is not significant. OVR was seen in 3/3 patients with AUC_{0-24h} greater than

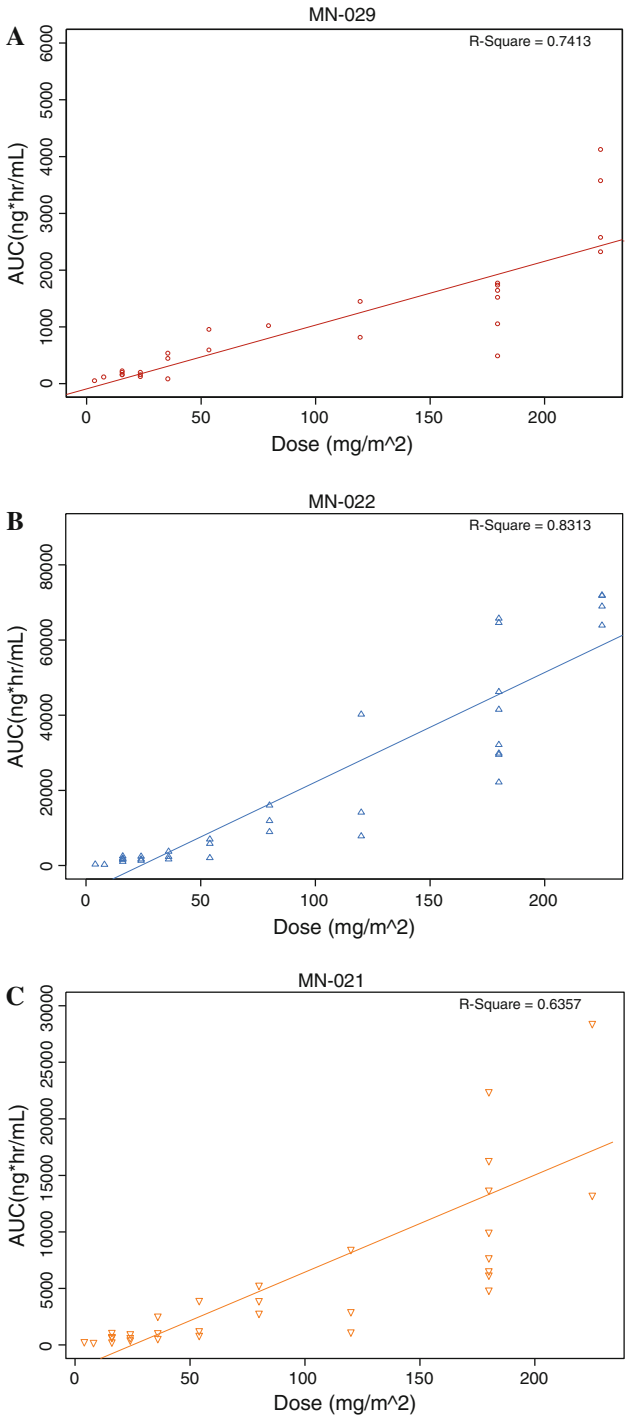

Fig. 1 **a** Linear regression analysis of MN-029 plasma area under the curve from time 0 to infinity ($AUC_{0-\infty}$) versus dose profiles in patients assessable for pharmacokinetic evaluation. **b** Linear regression analysis of MN-022 plasma area under the curve from time 0 to infinity ($AUC_{0-\infty}$) versus dose profiles in patients assessable for pharmacokinetic evaluation. **c** Linear regression analysis of MN-021 plasma area under the curve from time 0 to infinity ($AUC_{0-\infty}$) versus dose profiles in patients assessable for pharmacokinetic evaluation

2,000 ng h/mL, in 3/11 patients with AUC_{0-24h} between 700 and 2,000 ng h/mL, and 0/10 patients with AUC_{0-24h} less than 700 ng h/mL.

Discussion

Targeted destruction of the established tumor vasculature is a relatively novel anti-tumor strategy. There is substantial support for this approach in animal models and hints of efficacy in some early clinical trials [10, 11, 26–28]. It is important to note that the inhibitory effect of MN-029 and MN-022 on tubulin polymerization in vitro, as well as that for combretastatin (another VDA), occurs within minutes, but begins to diminish over a 60-min period [18]. Thus, unlike cytotoxic tubulin-binding agents such as colchicine, vincristine, and vinblastine, the binding of MN-029 and MN-022 to tubulin appears to be short lived, which could explain its ability to target and disrupt tumor vasculature without overt cytotoxic effects on normal tissues and vessels. Nevertheless, the toxicity profile for VDAs is suggestive of vascularly active agents and includes reports of acute coronary syndromes and other thromboembolic events, alterations in hemodynamic and electrophysiologic parameters (e.g., blood pressure, ventricular conduction and heart rate), transient flush, and tumor as well as abdominal pain [11, 27–30]. Neurotoxicity has also been reported [27, 28].

MN-029 administered every 3 weeks was generally well tolerated. The most common toxicities were mild or moderate and manageable with outpatient care. There was a lack of traditional cytotoxic side effects (e.g., myelosuppression, mucositis, and alopecia). Of note, there was no overt evidence of cumulative toxicity. Even though it is always difficult to evaluate cumulative effects in the phase I setting, it is worth mentioning that 53% of the patients in this study completed 3 courses of therapy and that 17 patients were dose escalated (Table 2). Serious toxicities were seen at 225 mg/m^2 and consisted of grade 3 transaminitis and a transient ischemic attack. Both patients recovered from the event without sequelae. One out of 8 new patients experienced a cardiovascular DLT at 180 mg/m^2. The event was interpreted as a possible reversible episode of acute coronary ischemia, with preservation of myocardial function, perhaps due to coronary vasospasm. No cardiovascular abnormalities were noted by the patient or investigator in real time, and the ECG changes did not result in changes in left ventricular function or show focal wall motion abnormalities on a follow-up echocardiogram. An exercise stress test confirmed normal exercise tolerance

Table 5 Tumor characteristics and acute change in vascular parameters (6–8 h post-dose) in all patients with evaluable dynamic contrast-enhanced magnetic resonance imaging

Patient no.	Tumor type	Target lesion location	Original dose (mg/m^2)	K^{trans}			$IAUCBN_{90}$		
				Pre-dose	Post-dose	%Δ	Pre-dose	Post-dose	%Δ
Low doses									
02-001	Renal cell carcinoma	Liver	16	0.018	0.018	0	0.34	0.34	0
02-002	Hepatocellular carcinoma	Liver	16	0.018	0.017	−5.5	0.32	0.30	−6.3
01-003	Urethral carcinoma	Pelvis	16	0.0083	0.0093	12	0.21	0.25	19
01-005	Colorectal cancer	Liver	24	0.010	0.013	30	0.20	0.24	20
01-006	Renal cell carcinoma	Liver	24	0.0063	0.0083	31.7	0.13	0.15	15.4
01-007	Melanoma	Pelvis	36	0.016	0.017	6.3	0.30	0.34	13.3
02-005	Renal cell carcinoma	Retroperitoneum	36	0.021	0.020	−4.8	0.37	0.34	8.1
01-008	Renal cell carcinoma	Abdominal wall	54	0.023	0.025	8.7	0.42	0.45	7.1
02-007	Gastrinoma	Liver	54	0.012	0.012	0	0.22	0.22	0
01-009	Colorectal cancer	Pelvis	54	0.024	0.027	12.5	0.48	0.55	14.6
Intermediate dose									
02-008	Colorectal cancer	Rectal mass	80	0.021	0.024	14.3	0.10	0.16	60
01-010	Adenocarcinoma UPS	Abdominal mass	80	0.019	0.019	0	0.09	0.09	0
Biologically active doses									
02-010[a]	Renal cell carcinoma	Lung	120	0.032	0.029	−9.4	0.25	0.22	−12
02-010[a]		Lung	120	0.019	0.013	−31.6	0.15	0.11	−26.7
02-011	Colorectal cancer	Liver	120	0.042	0.037	−11.9	0.31	0.19	−38.7
01-012	Soft-tissue sarcoma	Peritoneum	120	0.019	0.014	−26.3	0.11	0.052	−52.7
02-012	NSCLC	Liver	180	0.028	0.027	−3.6	0.23	0.21	−8.7
02-013	Colorectal cancer	Liver	180	0.025	0.028	12	0.16	0.20	25
01-014	Pancreatic cancer	Peritoneum	180	0.019	0.017	−10.5	0.099	0.095	−4
02-014	Hepatocellular carcinoma	Pelvis	180	0.020	0.015	−25	0.36	0.28	−22.2
01-015	Melanoma	Pelvis	180	0.007	0.0044	−37.1	0.16	0.10	−37.5
02-015	Colorectal cancer	Liver	225	0.018	0.013	−27.8	0.32	0.25	−21.9
01-016[a]	Colorectal cancer	Lung	225	0.012	0.011	−8.3	0.15	0.13	−13.3
01-016[a]		Lung	225	0.013	0.0093	−28.5	0.13	0.11	−15.4
02-018	Soft-tissue sarcoma	Inguinal	180	0.014	0.013	−7.1	0.25	0.24	−4
02-019[a]	Carcinoid tumor	Liver	180	0.013	0.014	7.7	0.13	0.13	0
02-019[a]		Liver	180	0.014	0.013	−7.1	0.16	0.15	−6.25

K^{trans}: volume transfer constant between blood plasma and extra-cellular, extra-vascular space, rounded to 3 decimals; $IAUCBN_{90}$: blood-normalized area under the tumor enhancement curve over the first 90 s post-injection, rounded to 2 decimals; %Δ: percent change, due to rounding these values do not completely match those in Fig. 1c, d

NSCLC non-small cell lung cancer, *UPS* unknown primary site

[a] Two analyzable lesions were present for these patients

with no exercise-induced ischemia. Taking all these results into account, the recommended phase II dose (RP2D) was considered to be 180 mg/m^2.

It has been determined from preclinical studies that VDAs can induce vascular shutdown within tumors at doses less than one-tenth of the MTD used in murine models [10, 26]. However, as previously stated, important observations have emerged from early clinical trials of other VDAs which indicate that these compounds may not be completely tumor selective [11, 12, 28–32]. Consequently, a potential explanation would be that targeting the tumor vasculature can induce transient changes in normal vascular compartments, causing the observed clinical presentations. The blood flow deficit must not have lasted long, since these presentations were not associated with permanent tissue injury.

MN-029 plasma levels decreased in a multi-exponential manner. The mean apparent $t_{1/2}$ (based on blood sampling up to 24 h) appeared to be dependent on dose. However, inter-patient variation in pharmacokinetics was large, as

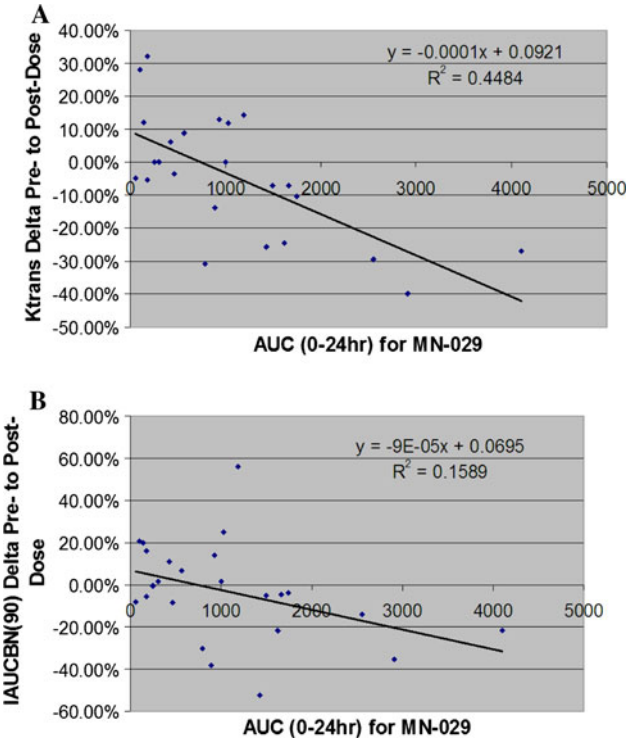

Fig. 2 **a** Scatter plot comparing AUC_{0-24h} (ng h/mL) for MN-029 to percentage change in K^{trans} from baseline to 6–8 h post-dose for each of the 24 evaluable patients. **b** Scatter plot comparing AUC_{0-24h} (ng h/mL) for MN-029 to percentage change in $IAUCBN_{90}$ from baseline to 6–8 h post-dose for each of the 24 evaluable patients

shown in Fig. 1a–c. MN-029 C_{max} and $AUC_{0-\infty}$ values increased with increasing doses and the $AUC_{0-\infty}$ appeared to be dose proportional. The clearance of MN-029 did not appear to decrease with increasing dose (Table 4). The conversion of MN-029 to MN-022 was rapid. The $AUC_{0-\infty}$ for both metabolites were greater than those of MN-029.

There were no objective responses, but five patients had sustained stable disease (≥6 months) at the data cut-off date. This finding must be interpreted with caution, considering the indolent nature of some tumor types, like carcinoid tumor. Nevertheless, a cytostatic effect is a postulated outcome of VDA therapy. Of note, one patient with this histology had symptomatic improvement. Several preclinical studies have shown that VDA-treated tumors can re-grow from a characteristic rim of residual viable cells at the tumor periphery [10, 33]. A rapid, reactive mobilization and subsequent tumor homing of circulating endothelial cells (CECs) can contribute to this re-growth [34]. This might prevent significant activity of VDAs as monotherapy, reinforcing the concept of combination therapy to obtain cytoreduction [17]. CECs are being evaluated as biomarkers of vascular damage and efficacy for antiangiogenic therapy [35–37]. In a phase I study of ZD6126, the quantification of CECs showed a peak level at 4 h post-dose and suggested increasing vascular damage after repeat dosing [29]. Measurement of CECs, with a particular emphasis on subpopulation kinetics and apoptotic status, could be of value in the evaluation of VDAs in the clinic [38–41]. Combinations of VDAs with VEGF inhibitors seem to be mechanistically appropriate [42].

Percent CoV for K^{trans} and $IAUCBN_{90}$ in this study were 8.7 and 8.8%, respectively. These values are consistent with those that have been obtained previously using this analysis system [43] and were used to inform the assessment of OVR for individual subjects in this study. The scan-rescan reproducibility values generated using the ten low-dose patients are in close accord with those that have been generated in other studies making use of a data-derived arterial input function [22, 43, 44]. This is an important point, in that the scan–rescan reproducibility of the measurement technique is the primary driver of the number of patients required in a given cohort in order to achieve statistically significant demonstration of rapid decrease in tumor vascular parameters for a given mean reduction in K^{trans} or $IAUCBN_{90}$ [43]. It is also helpful to observe that there is no apparent difference in reproducibility between the model-based K^{trans} and the more heuristic $IAUCBN_{90}$. Six of the twelve patients receiving doses of MN-029 ≥120 mg/m^2 achieved OVR in at least one of their target lesions. This is a strong indication that a dose-dependent treatment effect is present in this study. This conclusion is bolstered by the observation that there was a statistically significant difference between the low-dose and the biologically active dose groups in terms of changes in both K^{trans} and $IAUCBN_{90}$ and by the fact that the high ends of the 95% confidence intervals for change in the biologically active dose group for both parameters were less than 0. K^{trans} and AUC_{0-24h} for MN-029 are negatively correlated ($R^2 = 0.45$, $P < 0.001$; Fig. 1c).

Other VDAs are advanced in clinical development, particularly fosbretabulin (combretastatin-A4 phosphate) that is being evaluated in randomized phase II/III studies [45]. The addition of fosbretabulin to standard doses of chemotherapy and bevacizumab seems to be tolerable, but there were three reversible cardiac ischemia events in patients with non-small cell lung cancer [46, 47]. The reported adverse events of MN-029 appear to reveal the class effect profile of VDAs, although there were no reports of transient hypertension, syncope, QTc prolongation, or neurotoxicity in this study [45]. This safety profile is preliminary, and further clinical studies are required to confirm the absence of these sporadic adverse events reported with vascular-disrupting therapy. Another phase I study

evaluated MN-029 when administered every week for three consecutive weeks out of four and also determined a RP2D of 180 mg/m^2 (this contemporaneous study stopped dose escalation after our findings) [48]. Of note, this triple-dose intensity did not translate in greater or different toxicities, suggesting that the schedule of administration of VDAs warrants further evaluation.

In conclusion, MN-029 (denibulin HCl) once every 3 weeks was generally well tolerated at doses up to and including 180 mg/m^2. Concentrations yielding vascular shutdown in preclinical experiments were achieved, and DCE-MRI showed acute decrease in tumor vascular parameters at doses of MN-029 $\geq$ 120 mg/m^2. An accelerated, intra-patient dose-escalation design was successfully implemented. This is the first-in-human study of MN-029 and provides a basis for additional studies, including combination with conventional treatment. Appropriate patient selection and close cardiovascular monitoring, as instituted in this study, are suggested in further development of MN-029.

Acknowledgments We thank Ana Ruiz-Garcia and Louis Lazo Radulovic for helpful discussions and technical assistance. This work was supported by MediciNova, Inc.

Conflicts of interest Alejandro D Ricart is compensated as an employee of Pfizer Inc and owns stock/stock options in Pfizer Inc. Edward A. Ashton, Matthew M. Cooney, John Sarantopoulos, Joanna M. Brell, Gerardo Medina, Angela Zambito: no disclosures. Maria A. Feldman, Kale E. Ruby, Kazuko Matsuda, Mark S. Munsey are compensated as employees of MediciNova Inc. Anthony W. Tolcher's institution has received research funding from Abbott, Ambit, Amgen, Array BioPharma, Astellas, AVEO/Schering/Plough, Azaya Therapeutics, Bayer, Biogen Idec, BiPar, Bristol-Myers Squibb, Calando, Cougar, Dendreon, Eli Lilly, Enzon, Exelixis, Five Prime, Genentech, Genta, Glaxo Smith Kline, Hana Biosciences, Hoffman-La Roche, Merck, Merrimack, MethylGene, Myriad, Nektar, Nerviano, Proteolix, Sanofi-Aventis, Spectrum, Symphogen; he has also received payment for consulting and advisory agreements from Abbott, Abgenomics, Abraxis, ACT Biotech, Actavis, Adnexus, Adventrx Pharmaceuticals, Ambit, Amgen, Ariad Pharmaceuticals, Arresto Biosciences, Astellas, AstraZeneca, AVEO, Bayer, Bind Bio, Biogen Idec, BiPar, Calando, Calistoga, Chemokine, Curis, Daiichi Sankyo, Dendreon, Dicerna, Eli Lilly, EMTx, Endo, Enzon, Exelixis, Five Prime, Genentech, Genta, Geron, Glaxo Smith Kline, HUYA Bioscience, Intellikine, Johnson & Johnson, Merck, MethylGene, Micromet, Myriad, Nektar, Nerviano, Neumedicines, Onyx, Otsuka, Pfizer, ProNai, Regeneron, Sanofi-Aventis, Santaris, Schering Plough, Seattle Genetics, Semophore, Spectrum, Supergen, Symphogen, Vaccinex, and Veeda. Scot C. Remick has received a clinical research grant from MediciNova Inc.

Appendix

See Table 6.

Table 6 Validated LC–MS/MS method summary for the simultaneous quantitation of MN-029, MN-022, and N-acetyl MN-022 in human plasma

Anticoagulant	Sodium heparin
Preservative	Amastatin hydrochloride (20 μM)
Assay volume required	100 μL
Detection method	Positive ion/MRM
Standard curve range	
MN-029	0.2–150 ng/mL
MN-022	0.2–150 ng/mL
N-Acetyl MN-022	0.2–150 ng/mL
QC	
MN-029	0.2, 0.6, 60, 120 ng/mL
MN-022	0.2, 0.6, 60, 120 ng/mL
N-Acetyl MN-022	0.2, 0.6, 60, 120 ng/mL
Regression type	
MN-029	Linear ($1/x^2$ weighting factor)
MN-022	Linear ($1/x^2$ weighting factor)
N-Acetyl MN-022	
Quantitation method	Peak area ratio
Precision (%CV) and accuracy (%RE)	
MN-029	Precision: 5.5–11.3%; accuracy: −2.0 to 5.0%
MN-022	Precision: 6.0–9.3%; accuracy: −6.5 to 0.8%
N-Acetyl MN-022	Precision: 6.1–7.8%; accuracy: −8.8 to −2.3%

References

1. Hurwitz H, Fehrenbacher L, Novotny W et al (2004) Bevacizumab plus irinotecan, fluorouracil, and leucovorin for metastatic colorectal cancer. N Engl J Med 350:2335–2342
2. Ratain MJ, Eisen T, Stadler WM et al (2006) Phase II placebo-controlled randomized discontinuation trial of sorafenib in patients with metastatic renal cell carcinoma. J Clin Oncol 24:2505–2512
3. Motzer RJ, Hutson TE, Tomczak P et al (2007) Sunitinib versus interferon alfa in metastatic renal-cell carcinoma. N Engl J Med 356:115–124
4. Sandler A, Gray R, Perry MC et al (2006) Paclitaxel-carboplatin alone or with bevacizumab for non-small-cell lung cancer. N Engl J Med 355:2542–2550
5. Siemann DW, Bibby MC, Dark GG et al (2005) Differentiation and definition of vascular-targeted therapies. Clin Cancer Res 11:416–420
6. Thorpe PE (2004) Vascular targeting agents as cancer therapeutics. Clin Cancer Res 10:415–427
7. Cooney MM, van Heeckeren W, Bhakta S et al (2006) Drug insight: vascular disrupting agents and angiogenesis–novel approaches for drug delivery. Nat Clin Pract Oncol 3:682–692
8. Thorpe PE, Chaplin DJ, Blakey DC (2003) The first international conference on vascular targeting: meeting overview. Cancer Res 63:1144–1147
9. Tozer GM, Prise VE, Wilson J et al (2001) Mechanisms associated with tumor vascular shut-down induced by combretastatin

A-4 phosphate: intravital microscopy and measurement of vascular permeability. Cancer Res 61:6413–6422
10. Davis PD, Dougherty GJ, Blakey DC et al (2002) ZD6126: a novel vascular-targeting agent that causes selective destruction of tumor vasculature. Cancer Res 62:7247–7253
11. Dowlati A, Robertson K, Cooney M et al (2002) A phase I pharmacokinetic and translational study of the novel vascular targeting agent combretastatin a-4 phosphate on a single-dose intravenous schedule in patients with advanced cancer. Cancer Res 62:3408–3416
12. Galbraith SM, Rustin GJ, Lodge MA et al (2002) Effects of 5, 6-dimethylxanthenone-4-acetic acid on human tumor microcirculation assessed by dynamic contrast-enhanced magnetic resonance imaging. J Clin Oncol 20:3826–3840
13. Galbraith SM, Maxwell RJ, Lodge MA et al (2003) Combretastatin A4 phosphate has tumor antivascular activity in rat and man as demonstrated by dynamic magnetic resonance imaging. J Clin Oncol 21:2831–2842
14. Collins JM (2003) Functional imaging in phase I studies: decorations or decision making? J Clin Oncol 21:2807–2809
15. Evelhoch JL, LoRusso PM, He Z et al (2004) Magnetic resonance imaging measurements of the response of murine and human tumors to the vascular-targeting agent ZD6126. Clin Cancer Res 10:3650–3657
16. Parkins CS, Dennis MF, Stratford MR et al (1995) Ischemia reperfusion injury in tumors: the role of oxygen radicals and nitric oxide. Cancer Res 55:6026–6029
17. Horsman MR, Siemann DW (2006) Pathophysiologic effects of vascular-targeting agents and the implications for combination with conventional therapies. Cancer Res 66:11520–11539
18. MN-029 Investigator's brochure in Medicinova Inc (2004)
19. Shi W, Siemann DW (2005) Preclinical studies of the novel vascular disrupting agent MN-029. Anticancer Res 25:3899–3904
20. Simon R, Freidlin B, Rubinstein L et al (1997) Accelerated titration designs for phase I clinical trials in oncology. J Natl Cancer Inst 89:1138–1147
21. Therasse P, Arbuck SG, Eisenhauer EA et al (2000) New guidelines to evaluate the response to treatment in solid tumors. European Organization for Research and Treatment of Cancer, National Cancer Institute of the United States, National Cancer Institute of Canada. J Natl Cancer Inst 92:205–216
22. Ashton E, McShane T, Evelhoch J (2005) Inter-operator variability in perfusion assessment of tumors in MRI using automated AIF detection. LNCS 3749:451–458
23. Johnson NL, Kotz S, Balakrishnan N (1994) Continuous univariate distributions. Wiley, New York, pp 127–129
24. Leach M, Brindle K, Evelhoch J et al (2005) The assessment of antiangiogenic and antivascular therapies in early-stage clinical trials using magnetic resonance imaging: issues and recommendations. Br J Cancer 92:1599–1610
25. Evelhoch J (1999) Key factors in the acquisition of contrast kinetic data for oncology. J Magn Reson Imaging 10:254–259
26. Dark GG, Hill SA, Prise VE et al (1997) Combretastatin A-4, an agent that displays potent and selective toxicity toward tumor vasculature. Cancer Res 57:1829–1834
27. Jameson MB, Thompson PI, Baguley BC et al (2003) Clinical aspects of a phase I trial of 5, 6-dimethylxanthenone-4-acetic acid (DMXAA), a novel antivascular agent. Br J Cancer 88:1844–1850
28. Rustin GJ, Galbraith SM, Anderson H et al (2003) Phase I clinical trial of weekly combretastatin A4 phosphate: clinical and pharmacokinetic results. J Clin Oncol 21:2815–2822
29. Beerepoot LV, Radema SA, Witteveen EO et al (2006) Phase I clinical evaluation of weekly administration of the novel vascular-targeting agent, ZD6126, in patients with solid tumors. J Clin Oncol 24:1491–1498
30. van Heeckeren WJ, Bhakta S, Ortiz J et al (2006) Promise of new vascular-disrupting agents balanced with cardiac toxicity: is it time for oncologists to get to know their cardiologists? J Clin Oncol 24:1485–1488
31. Anderson HL, Yap JT, Miller MP et al (2003) Assessment of pharmacodynamic vascular response in a phase I trial of combretastatin A4 phosphate. J Clin Oncol 21:2823–2830
32. Cooney MM, Radivoyevitch T, Dowlati A et al (2004) Cardiovascular safety profile of combretastatin a4 phosphate in a single-dose phase I study in patients with advanced cancer. Clin Cancer Res 10:96–100
33. Chaplin DJ, Hill SA (2002) The development of combretastatin A4 phosphate as a vascular targeting agent. Int J Radiat Oncol Biol Phys 54:1491–1496
34. Shaked Y, Ciarrocchi A, Franco M et al (2006) Therapy-induced acute recruitment of circulating endothelial progenitor cells to tumors. Science 313:1785–1787
35. Mancuso P, Colleoni M, Calleri A et al (2006) Circulating endothelial-cell kinetics and viability predict survival in breast cancer patients receiving metronomic chemotherapy. Blood 108:452–459
36. Willett CG, Boucher Y, di Tomaso E et al (2004) Direct evidence that the VEGF-specific antibody bevacizumab has antivascular effects in human rectal cancer. Nat Med 10:145–147
37. Solovey A, Lin Y, Browne P et al (1997) Circulating activated endothelial cells in sickle cell anemia. N Engl J Med 337:1584–1590
38. Beerepoot LV, Mehra N, Vermaat JS et al (2004) Increased levels of viable circulating endothelial cells are an indicator of progressive disease in cancer patients. Ann Oncol 15:139–145
39. Mancuso P, Burlini A, Pruneri G et al (2001) Resting and activated endothelial cells are increased in the peripheral blood of cancer patients. Blood 97:3658–3661
40. Monestiroli S, Mancuso P, Burlini A et al (2001) Kinetics and viability of circulating endothelial cells as surrogate angiogenesis marker in an animal model of human lymphoma. Cancer Res 61:4341–4344
41. Shaked Y, Bertolini F, Man S et al (2005) Genetic heterogeneity of the vasculogenic phenotype parallels angiogenesis; implications for cellular surrogate marker analysis of antiangiogenesis. Cancer Cell 7:101–111
42. Shi W, Siemann DW (2005) Targeting the tumor vasculature: enhancing antitumor efficacy through combination treatment with ZD6126 and ZD6474. In Vivo 19:1045–1050
43. Ashton E, Raunig D, Ng C et al (2008) Scan-rescan variability in perfusion assessment of tumors in MRI using both model and data-derived arterial input function. J Magn Reson Imaging 28:791–796
44. Rijpkema M, Kaanders J, Joosten F et al (2001) Method for quantitative mapping of dynamic MRI contrast agent enhancement in human tumors. J Magn Reson Imaging 14:457–463
45. Siemann DW, Chaplin DJ, Walicke PA (2009) A review and update of the current status of the vasculature-disabling agent combretastatin-A4 phosphate (CA4P). Expert Opin Investig Drugs 18:189–197
46. Garon EB, Kabbinavar FF, Neidhart JA et al. (2010) Randomized phase II trial of a tumor vascular disrupting agent fosbretabulin tromethamine (CA4P) with carboplatin (C), paclitaxel (P), and bevacizumab (B) in stage IIIb/IV nonsquamous non-small cell lung cancer (NSCLC): The FALCON trial. J Clin Oncol 28:7s (abstr 7587)
47. Nathan PD, Judson I, Padhani A et al. (2008) A phase I study of combretastatin A4 phosphate (CA4P) and bevacizumab in subjects with advanced solid tumors. J Clin Oncol 26 (abstr 3550)
48. Traynor AM, Gordon MS, Alberti D et al (2010) A dose escalation, safety, and tolerability study of MN-029 in patients with advanced solid tumors. Invest New Drugs 28:509–515